Substrate Selectivity in the Low Temperature Atomic Layer Deposition of Cobalt Metal Films from Bis(1,4-Di- Tert -Butyl-1,3-Diazadienyl)Cobalt and Formic Acid

UT Dallas Author(s):

Joseph P. Klesko
Sara M. Rupich
Yves. J. Chabal

Citation:

Kerrigan, M. M., J. P. Klesko, S. M. Rupich, C. L. Dezelah, et al. 2017. "Substrate selectivity in the low temperature atomic layer deposition of cobalt metal films from bis(1,4-di- tert -butyl-1,3-diazadienyl)cobalt and formic acid." Journal of Chemical Physics 146(5), doi:10.1063/1.4968848

Substrate selectivity in the low temperature atomic layer deposition of cobalt metal films from bis(1,4-di-*tert*-butyl-1,3-diazadienyl)cobalt and formic acid

Marissa M. Kerrigan,[1] Joseph P. Klesko,[1,2] Sara M. Rupich,[2] Charles L. Dezelah,[3] Ravindra K. Kanjolia,[3] Yves J. Chabal,[2] and Charles H. Winter[1,a)]
[1]*Department of Chemistry, Wayne State University, Detroit, Michigan 48202, USA*
[2]*Department of Materials Science and Engineering, University of Texas at Dallas, Richardson, Texas 75080-3021, USA*
[3]*EMD Performance Materials, 1429 Hilldale Ave, Haverhill, Massachusetts 01832, USA*

(Received 11 September 2016; accepted 14 November 2016; published online 1 December 2016)

The initial stages of cobalt metal growth by atomic layer deposition are described using the precursors bis(1,4-di-*tert*-butyl-1,3-diazadienyl)cobalt and formic acid. Ruthenium, platinum, copper, Si(100), Si–H, SiO_2, and carbon-doped oxide substrates were used with a growth temperature of 180 °C. On platinum and copper, plots of thickness versus number of growth cycles were linear between 25 and 250 cycles, with growth rates of 0.98 Å/cycle. By contrast, growth on ruthenium showed a delay of up to 250 cycles before a normal growth rate was obtained. No films were observed after 25 and 50 cycles. Between 100 and 150 cycles, a rapid growth rate of ∼1.6 Å/cycle was observed, which suggests that a chemical vapor deposition-like growth occurs until the ruthenium surface is covered with ∼10 nm of cobalt metal. Atomic force microscopy showed smooth, continuous cobalt metal films on platinum after 150 cycles, with an rms surface roughness of 0.6 nm. Films grown on copper gave rms surface roughnesses of 1.1–2.4 nm after 150 cycles. Films grown on ruthenium, platinum, and copper showed resistivities of <20 $\mu\Omega$ cm after 250 cycles and had values close to those of the uncoated substrates at ≤150 cycles. X-ray photoelectron spectroscopy of films grown with 150 cycles on a platinum substrate showed surface oxidation of the cobalt, with cobalt metal underneath. Analogous analysis of a film grown with 150 cycles on a copper substrate showed cobalt oxide throughout the film. No film growth was observed after 1000 cycles on Si(100), Si–H, and carbon-doped oxide substrates. Growth on thermal SiO_2 substrates gave ∼35 nm thick layers of cobalt(II) formate after ≥500 cycles. Inherently selective deposition of cobalt on metallic substrates over Si(100), Si–H, and carbon-doped oxide was observed from 160 °C to 200 °C. Particle deposition occurred on carbon-doped oxide substrates at 220 °C. *Published by AIP Publishing.* [http://dx.doi.org/10.1063/1.4968848]

I. INTRODUCTION

Cobalt metal films have increasing importance as magnetic materials,[1,2] precursors to $CoSi_2$ contacts,[3] liners and caps of copper features in microelectronics devices,[4–9] and possibly even as copper replacement conductors.[10] Cobalt metal films have been deposited by physical deposition[11–13] and chemical vapor deposition (CVD) using molecular cobalt precursors.[14–20] The push to decrease dimensions to <10 nm in microelectronics devices necessitates cobalt metal growth by atomic layer deposition (ALD) to satisfy conformality and thickness requirements.[21–23] ALD can provide perfect conformality and sub-nm thickness control because of the inherent self-limited growth mechanism.[21–23] Plasma-enhanced ALD of cobalt metal films has been described using a range of organometallic cobalt precursors with various reducing plasma species.[24–33] However, plasmas can damage substrates and can also give poor conformal coverage in high aspect ratio features because of the hydrogen atom recombination on the substrate surface.[34] There are few reports describing the thermal ALD of cobalt metal films. The amidinate precursor $Co(iPrNCMeNiPr)_2$ was employed with H_2 at 350 °C and gave a growth rate of 0.12 Å/cycle.[35–39] $Co(iPrNCMeNiPr)_2$ was also used for cobalt metal ALD at 300-350 °C with H_2 or NH_3 as the co-reactants.[40–42] Although self-limited growth was established for $Co(iPrNCMeNiPr)_2$,[35] the deposition temperatures are substantially higher than the decomposition temperature of this precursor (215-225 °C),[15,37] implying a CVD contribution to the film growth. Cobalt metal films were grown using (2-*tert*-butylallyl)$Co(CO)_3$ and 1,1-dimethylhydrazine at 140 °C, but self-limited ALD growth was not confirmed.[43] Self-limited cobalt metal ALD was reported with the precursors $Co((Me)(iPr)COCNtBu)_2$ and $BH_3(NHMe_2)$ at a temperature of 180 °C, but the growth rate was 0.07 Å/cycle and deposition only occurred on a ruthenium substrate after a nucleation step.[44]

There is a considerable current interest in area-selective ALD, since selective deposition on the desired regions of patterned surfaces can reduce or eliminate the need for complex lithography and etching steps in traditional patterning.[45] Recent reports have described various approaches to enable

a)Author to whom correspondence should be addressed. Electronic mail: chw@chem.wayne.edu.

the selective ALD of metal films. Selective fluorination of only the horizontal surfaces in silicon fin array nanostructures allowed platinum ALD to proceed on the non-fluorinated vertical surfaces, while platinum ALD on the horizontal surfaces was inhibited for about 500 cycles.[46] In the ALD growth of tungsten metal from WF_6 and SiH_4, the addition of H_2 during the WF_6 pulse inhibited the nucleation on SiO_2 surfaces, without changing the nucleation on silicon surfaces, thereby allowing selective tungsten growth on the silicon regions of patterned substrates.[47] Substrates containing both copper metal and SiO_2 regions were treated with octylphosphonic acid to create self-assembled monolayers only on the copper regions. Subsequent dielectric ALD growth occurred mostly on the SiO_2 regions, and the self-assembled monolayers on the copper regions with some dielectric deposits could be removed after the dielectric growth to afford pristine copper surfaces without affecting the dielectric-coated SiO_2 regions.[48] Copper metal films were selectively deposited on palladium surfaces using $Cu(tmhd)_2$ (tmhd = 2,2,6,6-tetramethylheptane-3,5-dionate) and H_2 from 135 to 230 °C, and no growth was observed after 100 cycles on SiO_2 and Si_3N_4 surfaces.[49] Self-assembled octadecyltrimethoxysilane-derived monolayers were patterned on the oxide substrate surfaces and were found to block the ALD growth of iridium[50] and ruthenium[51] metal films, whereas these metals grew in the areas of the substrates where there were no self-assembled monolayers. Recent reports have described various types of selective cobalt metal depositions. Octadecyltrichlorosilane-derived self-assembled monolayers were deposited on the Si(001) substrates containing SiO_2 surfaces, and these substrates were then subjected to the thermal ALD growth of cobalt metal films using $Co(iPrNCMeNiPr)_2$ and NH_3 or H_2 at 300-350 °C.[40–42] The self-assembled monolayers blocked the growth of ALD cobalt metal for up to 1000 cycles. Application of analogous plasma-based processes did not show any selective growth, due to the degradation of the self-assembled monolayers by the plasma gases.[40–42] Selective growth of cobalt metal was observed on Si–H substrates using (2-*tert*-butylallyl)$Co(CO)_3$ and 1,1-dimethylhydrazine at 140 °C, whereas no growth occurred on SiO_2 substrates under the same conditions.[43] The origin of the selective growth was attributed to the hydrosilylation-like reactivity of (2-*tert*-butylallyl)$Co(CO)_3$ with the Si–H surface, leading to exothermic Co–Si bond formation and effective nucleation. By contrast, the reaction of (2-*tert*-butylallyl)$Co(CO)_3$ with the SiO_2 surface is endothermic, and no film growth occurs.[43] Cobalt carbonyl precursors were found to deposit cobalt metal selectively by CVD on patterned copper surfaces that also contain dielectric surfaces.[5,52,53] A preclean process prior to the cobalt metal deposition improved the selective deposition on copper.

We recently reported the ALD growth of high quality cobalt metal films using bis(1,4-di-*tert*-butyl-1,3-diazadienyl)cobalt (**1**, Fig. 1) and formic acid as the precursors.[54] This process gave a high growth rate of 0.95 Å/cycle within the 170-180 °C ALD window and afforded low resistivity films (13–19 $\mu\Omega$ cm compared to 6.24 $\mu\Omega$ cm for bulk cobalt metal at 20 °C[55]). Significantly, cobalt metal growth occurred selectively on ruthenium and platinum substrates, and no cobalt metal growth was observed after 1000 cycles on Si(100), Si–H, and SiO_2 surfaces. Herein, we report detailed studies of ALD cobalt metal growth behavior with **1** and formic acid on both metal and dielectric surfaces. The results demonstrate the inherently selective growth of cobalt metal on metallic substrates such as ruthenium, platinum, and copper, no detectable film growth after 1000 cycles on Si(100), Si–H, and carbon-doped oxide (CDO) surfaces, and deposition of thin cobalt(II) formate layers on SiO_2 substrates.

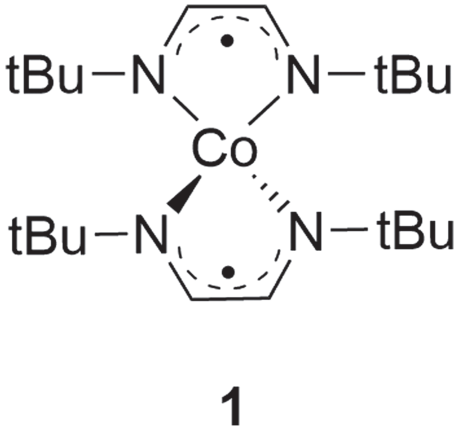

1

FIG. 1. Structure of precursor **1**.

II. EXPERIMENTAL

See the supplementary material for details relating to the ALD growth data and film characterization.

A Picosun R-75BE ALD reactor was used for the thin film deposition experiments. The ALD reactor was operated under a constant stream of nitrogen (99.9995%) at a pressure of 6-9 Torr. The deposition of Co metal thin films was studied with **1** and formic acid. Precursor **1** was prepared according to a literature procedure[56] and formic acid was purchased from Sigma Aldrich. In initial growth trials, the source temperature for **1** was found to be optimum at 130 °C under the reactor pressure. Substrate temperatures were varied between 160 and 240 °C. Nitrogen was used as both the carrier and purge gas and was purified from ambient air using a Texol GeniSys nitro-Generator. Film growth experiments used to assess selectivity were performed using the pulse sequence **1** (5.0 s)/N_2 purge (10.0 s)/formic acid (0.2 s)/N_2 purge (10.0 s) at 180 °C that was established in our previous report of cobalt metal ALD from **1** and formic acid.[54] For the selectivity temperature window experiments, the same pulse and purge sequence was used, but the deposition temperatures were varied as described below. ALD growth studies were performed on Ru (13 nm)/TaN (2 nm)/SiO_2 (100 nm)/Si(100), Cu (33 nm)/TaN (7 nm)/SiO_2 (100 nm)/Si(100), Pt (10 nm)/SiO_2 (100 nm)/Si(100), Si(100) with native oxide, Si–H, thermal SiO_2 (100 nm)/Si(100), and CDO (30-50 nm)/SiO_2 (100 nm)/Si(100) substrates. Si–H substrates were prepared by treating Si(100) with native oxide substrates with a 2% aqueous HF solution, followed by rinsing with deionized water, and then drying with a stream of clean, dry air. The other substrates were used as received, except that they were rinsed sequentially with isopropanol and deionized

water and then were dried with a stream of clean, dry air. One substrate of each kind, a 2 × 2 cm^2 coupon, was used in each experiment.

Film thicknesses were determined using cross-sectional scanning electron microscopy (SEM) collected on a JEOL-6510LV electron microscope. The growth rates were determined by dividing the measured film thicknesses by the number of deposition cycles. Film thicknesses were measured at a minimum of three positions on each film to evaluate the uniformity. Energy-Dispersive X-Ray Spectroscopy (EDS) was carried out on the JEOL-6510LV electron microscope using an Ametek EDAX system with Genesis Spectrum software. The accelerating voltage for the EDS measurements was 6 kV. Atomic force microscopy (AFM) measurements were conducted using a VEECO Dimension 3100 operated in the tapping mode. X-ray photoelectron spectroscopy (XPS) measurements were conducted using an Al K_α (1486.6 eV) X-ray source at a chamber base pressure of 10^{-10} Torr. Spectra were recorded using a 16-channel detector with a hemispherical analyzer. Sputtering was performed using argon ions supplied by an argon sputter gun positioned at a 45° angle with respect to the substrate normal. Each sample was sputtered over a 2 × 2 mm^2 area and measured over a 0.8 × 0.8 mm^2 area. Cobalt and copper metal standards were sputtered with 5 kV argon ions. An uncoated platinum substrate (Pt (10 nm)/SiO_2 (100 nm)/Si(100)) was used as a standard for platinum and was sputtered with 3 kV argon ions. The ALD-grown cobalt films on copper and platinum were sputtered with 3 kV argon ions. Sheet resistivity measurements were obtained using a Jandel 4-point probe in combination with a Keithley 2400 SourceMeter and a Keithley 2182A Nanovoltmeter. Infrared spectra were obtained on a Shimadzu IRTracer-100 spectrophotometer. All films grown on metal substrates passed the Scotch tape test.

III. RESULTS AND DISCUSSION

A. Film growth on ruthenium, platinum, and copper substrates

Fig. 2 shows the plots of thickness versus number of cycles for cobalt metal growth on ruthenium, platinum, and copper substrates at 180 °C for 25, 50, 100, 150, and 250 cycles using the growth conditions described above. For both platinum and copper surfaces, the plots were linear with growth rates of 0.98 Å/cycle. These values are within the experimental error of the 0.95 Å/cycle growth rate that we reported for the **1** and formic acid process on ruthenium substrates between 250 and 2000 cycles and at 1000 cycles on platinum and copper substrates.[54] Cobalt films grown with 25 cycles (~2.5 nm thick) can be measured with our electron microscope, but these thickness values have higher uncertainties than measurements made of thicker films. Accordingly, the presence of cobalt on the substrates was also probed qualitatively by EDS for films grown with 25, 50, and 100 cycles. All samples grown on platinum and copper substrates showed cobalt signals in the EDS spectra. The fact that the growth rates on platinum and copper substrates with 25–250 cycles are identical to those observed from 250 to 2000 cycles on ruthenium substrates and at 1000 cycles on platinum and copper,[54] coupled with the observation of cobalt signals in all of the EDS spectra, implies that the normal ALD growth occurs even at 25 cycles on platinum and copper substrates.

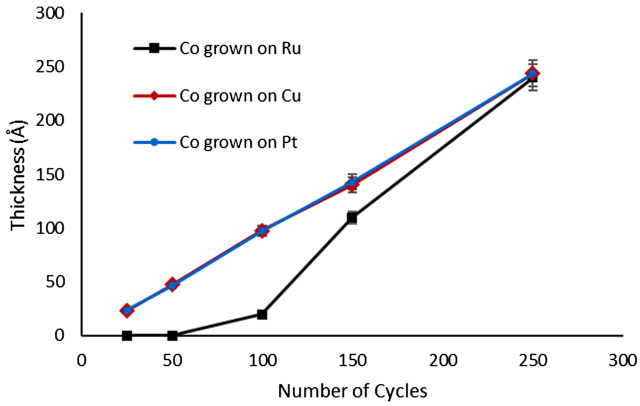

FIG. 2. Plots of thickness versus number of cycles for cobalt metal growth on ruthenium, platinum, and copper substrates at 180 °C.

In contrast to the linear growth behavior on platinum and copper substrates, cobalt growth on ruthenium substrates showed a delay at 180 °C of up to 250 cycles before the saturative growth rate ensued, beyond which a linear plot of thickness versus number of cycles was observed with a normal growth rate of 0.95 Å/cycle.[54] No detectable film growth (<2 nm) was observed by SEM after 25 and 50 growth cycles. After 100 cycles, a uniform thickness, ~2 nm continuous layer was observed by SEM. At 150 cycles, a ~10 nm thick cobalt film was observed. At 250 cycles and beyond, the normal 0.95 Å/cycle growth rate was obtained. Between 100 and 150 cycles on ruthenium substrates, the film thickness increased from ~2 nm to 10 nm, which corresponds to a growth rate of ~1.6 Å/cycle.[54] This value is much higher than the 0.95 Å/cycle growth rate observed between 250 and 2000 cycles on ruthenium substrates. In our previous paper, we reported that a CVD-like experiment conducted with **1** (5.0 s)/N_2 purge (10.0 s) and no formic acid pulses at 180 °C for 1000 cycles on a ruthenium substrate led to a film thickness of 13-15 nm.[54] For comparison, **1** undergoes thermal decomposition to cobalt metal in the solid state upon heating to ~235 °C and should thus be thermally stable at 180 °C.[56] Accordingly, it appears that there is a nucleation delay of about 100 cycles in the ALD growth process, during which no cobalt growth is observed by SEM (<2 nm). This delay may occur because of an oxidized ruthenium surface,[57] which could inhibit cobalt metal nucleation until treatment with **1** and formic acid can expose reactive surface sites. Between 100 and 150 cycles, the very high growth rate (~1.6 Å/cycle) suggests that the ruthenium/cobalt surface promotes the decomposition of **1** in a CVD-like fashion to afford a layer that covers the ruthenium surface (~10-15 nm). Once the ruthenium surface is covered by a cobalt layer (150-250 cycles), normal self-limited ALD growth ensues. It is not fully clear why the growth behavior on ruthenium substrates is different than that on platinum and copper substrates. However, nucleation in noble metal ALD processes is difficult, and many ruthenium ALD processes exhibit delays of up to several hundred cycles before normal growth ensues.[57] Factors that affect

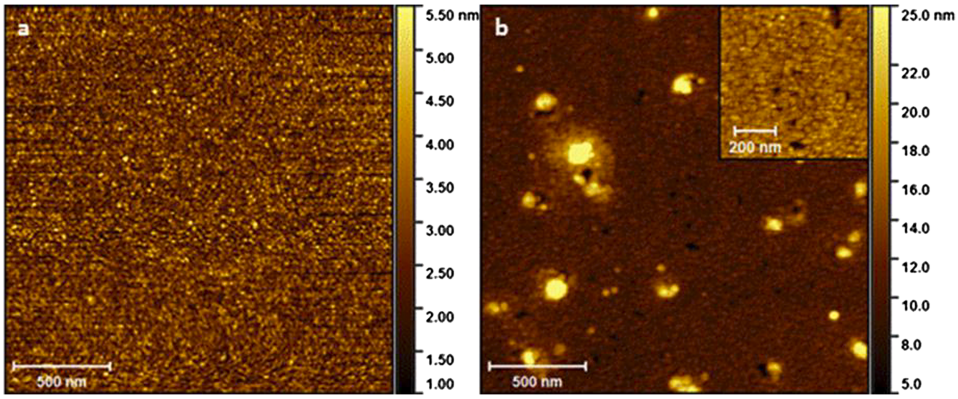

FIG. 3. AFM images of 15 nm of cobalt on (a) platinum and (b) copper. The inset shows a smooth region of the cobalt on copper film. Cobalt on platinum: rms = 0.6 nm. Cobalt on copper: rms = 2.4 nm, inset rms = 1.1 nm.

nucleation in noble metal ALD have been discussed, and surface treatments can affect nucleation.[57] In the present work, the ruthenium substrates were used as received and no pretreatments were carried out. Ruthenium surfaces are often oxidized,[57] which could affect cobalt metal nucleation. It is possible that various pretreatments of the ruthenium substrates could reduce or even eliminate the nucleation delay observed herein.

AFM was used to probe the surface topologies of films grown at 150 cycles (~14 nm thick) on platinum and copper substrates (Fig. 3). On platinum (Fig. 3(a)), the cobalt film had an rms surface roughness of 0.6 nm, compared to an rms surface roughness for the uncoated platinum substrate of 0.19 nm. This rms roughness corresponds to 4% of the film thickness and indicates a very smooth film. Fig. 3(b) shows the AFM image of the cobalt film on a copper substrate. The rms surface roughness for the full $2 \times 2\ \mu m^2$ region was 2.4 nm and was 1.1 nm for the inset showing a $0.7 \times 0.7\ \mu m^2$ region that did not contain any surface particles. For comparison, the rms value of the uncoated copper substrate was 0.69 nm. The surface contains widely spaced 30-125 nm diameter particles, as well as 30-60 nm diameter pits. The particles and pits originate from the copper substrates, since the AFM image of the uncoated substrates shows similar features. These surface features may originate from surface oxidation of the copper by air.[58] While AFM studies of thin cobalt films on ruthenium substrates were not carried out because of the nucleation delay at early growth stages, a 105 nm thick cobalt film on a ruthenium substrate grown at 180 °C had an rms surface roughness of 0.98 nm, compared to a value of 0.42 nm for the uncoated ruthenium substrate.[54] Accordingly, films grown from **1** and formic acid at 180 °C give very smooth films on ruthenium and platinum substrates. Films on copper substrates also have low rms surface roughnesses, although some pits and particles are observed due to the copper substrate.

The resistivities of the films grown on ruthenium, platinum, and copper substrates were measured for the samples grown from **1** and formic acid at 180 °C with 25, 50, 100, 150, and 250 cycles (Table I). On ruthenium, the resistivities range from 49 to 56 $\mu\Omega$ cm up to 100 cycles, which is similar to the resistivity value of the uncoated ruthenium substrates (~52 $\mu\Omega$ cm). The similarity of these resistivity values to that of the ruthenium substrate is consistent with the lack of observed film growth at 25 and 50 cycles. The slightly decreased resistivity at 100 cycles (49 $\mu\Omega$ cm) might correlate with the ~2 nm thick cobalt layer observed by SEM. At 150 cycles, the resistivity value decreased to 35.9 $\mu\Omega$ cm, which can be attributed to the ~10 nm thick cobalt layer. At 250 cycles, the resistivity dropped to 18.5 $\mu\Omega$ cm for the ~25 nm thick cobalt layer, which is within the 13–19 $\mu\Omega$ cm range observed for 95 nm thick ALD cobalt metal films grown at 180 °C from **1** and formic acid.[54] As noted above, normal ALD growth on ruthenium substrates begins at about 250 cycles. As a comparison, cobalt metal has a bulk resistivity of 6.24 $\mu\Omega$ cm at 20 °C.[55] For platinum substrates, the resistivity values of films grown with 25 (~2.5 nm thick layer) and 50 (~5 nm thick layer) cycles were 47.1 and 45.3 $\mu\Omega$ cm, which are close to that of the uncoated platinum substrate (~43 $\mu\Omega$ cm). Cobalt-platinum alloy films containing up to 55% platinum have room temperature resistivities between 45 and 52 $\mu\Omega$ cm, which are similar to the films grown with 25 and 50 cycles.[59] Accordingly, cobalt-platinum alloys cannot be ruled out at low film thicknesses (*vide infra*). At 100 cycles (~10 nm thick layer), the resistivity dropped to 34.3 $\mu\Omega$ cm, consistent with the thicker cobalt layer and more cobalt metal contributing to the resistivity. At 150 (~15 nm thick layer) and 250 (~25 nm thick layer) cycles, the resistivity values (20.1, 19.6 $\mu\Omega$ cm) were close to the 13–19 $\mu\Omega$ cm range observed for 95 nm thick cobalt metal films on ruthenium substrates that we reported

TABLE I. Resistivities of cobalt films on metallic substrates.

Number of cycles	Ruthenium[a,b]	Platinum[a,c]	Copper[a,d]
25	56.1	47.1	1.7
50	54.3	45.3	1.7
100	49.0	34.3	1.7
150	35.9	20.1	2.9
250	18.5	19.6	14.9

[a]Values are in $\mu\Omega$ cm.
[b]Resistivity of the uncoated ruthenium substrate is 52.1 $\mu\Omega$ cm.
[c]Resistivity of the uncoated platinum substrate is 42.6 $\mu\Omega$ cm.
[d]Resistivity of the uncoated copper substrate is 1.7 $\mu\Omega$ cm.

previously.[54] On copper substrates, the resistivities of films grown with 25 (~2.5 nm thick layer), 50 (~5 nm thick layer), and 100 (~10 nm thick layer) cycles were identical to those of the uncoated copper substrates (1.7 $\mu\Omega$ cm). This observation is consistent with the conduction occurring through the copper substrate in these thin films, formation of a highly conductive copper-cobalt alloy, or the presence of a thin surface copper layer (*vide infra*). The resistivity of the film grown at 150 cycles (~15 nm thick layer) increased slightly to 2.9 $\mu\Omega$ cm. At 250 cycles (~25 nm thick), the resistivity of the cobalt layer (14.9 $\mu\Omega$ cm) was within the 13–19 $\mu\Omega$ cm range noted above for 95 nm thick cobalt metal films on ruthenium substrates.

Films about 14 nm thick grown on copper and platinum substrates with 150 cycles of ALD cobalt at 180 °C were analyzed by XPS to gain insight into the nucleations and film properties. Both films gave the expected thicknesses for a growth rate of ~0.95 Å/cycle, consistent with normal ALD growth. The film on platinum showed oxidized cobalt in the scan prior to the argon ion sputtering, consistent with our earlier report on surface oxidation in cobalt metal films.[54] The carbon 1s ionizations in the as-deposited film were consistent with adventitious surface hydrocarbons and disappeared after 15 s of sputtering. The oxidized cobalt and oxygen ionizations disappeared after sputtering for 45 s, after which only cobalt metal was present. Upon sputtering for 15 s or longer, ionizations consistent with cobalt metal were observed (Co $2p_{3/2}$ 778.36 eV, Co $2p_{1/2}$ 793.46 eV). The oxygen level was 1.0% after sputtering for 75 s, and carbon and nitrogen levels were below the detection limits (<0.5%). For comparison, a cobalt metal standard sample showed Co $2p_{3/2}$ and Co $2p_{1/2}$ ionizations at 778.36 and 793.46 eV, respectively. The surface of the standard sample also showed oxidized cobalt, oxygen, and carbon ionizations prior to sputtering. Upon argon ion sputtering of the standard cobalt sample for 15 s, the oxygen and carbon ionizations disappeared, the oxidized cobalt was absent, and the cobalt metal ionizations were observed. Platinum ionizations were absent in the scan of the cobalt film on platinum before sputtering but appeared after 15 s of sputtering (Pt $4f_{7/2}$ 70.03 eV, Pt $4f_{5/2}$ 73.48 eV) and were identical to the binding energies observed for the platinum metal standard. These data are consistent with cobalt metal deposition on the platinum substrate, with some surface oxidation that likely occurs upon the exposure of the film to ambient atmosphere. Figure 4 shows the atomic concentrations of elements present in the film after various sputtering times. Notably, there is considerable intermixing of cobalt and platinum upon sputtering for 15 s or more. These data imply formation of an interfacial cobalt-platinum alloy, which likely contributes to the facile nucleation of the cobalt films on platinum substrates. The intermixing of cobalt and platinum increases throughout the 14 nm thick cobalt layer and possibly continues into the 10 nm thick platinum layer. In related studies, ALD copper films have been shown to form interfacial alloys that enhance nucleation on palladium and platinum substrates but not on ruthenium substrates.[60–62]

14 nm thick cobalt films grown on copper substrates were also studied by XPS. Unlike the cobalt films on platinum, XPS showed oxidized cobalt throughout the film with underlying copper metal. Ionizations from cobalt metal were absent or of very low intensity. These data are consistent with complete

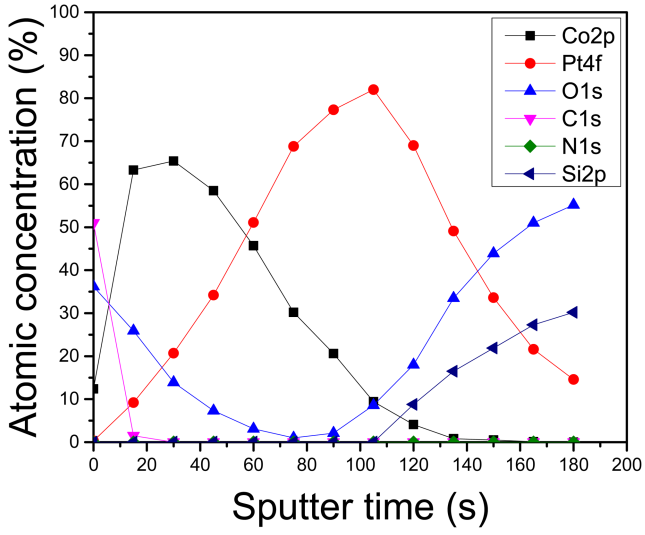

FIG. 4. Plot of atomic concentration versus argon ion sputtering time of a 14 nm thick cobalt film grown on a platinum substrate at 180 °C.

oxidation of the cobalt film upon exposure to ambient atmosphere. Metallic copper is well known to undergo surface oxidation upon exposure to air.[58] A copper metal standard sample also showed surface oxidation, which disappeared upon sputtering for 15 s. It is possible that the oxidized copper on the substrate surface is reduced by the growing cobalt metal film, resulting in copper metal and cobalt oxide. Cobalt metal that grows on top of the cobalt oxide interfacial layer would be oxidized to cobalt oxide upon exposure to ambient air. Figure 5 shows the atomic concentrations of elements present in the film after various sputtering times. The oxygen and cobalt concentrations are similar throughout the film, consistent with the presence of cobalt oxide. Carbon and nitrogen levels were below the detection limits (<0.5%) after 60 s of sputtering. As above, there is a considerable intermixing of the copper and cobalt layers. It is possible that the nucleation mechanism entails reaction of the surface copper oxides

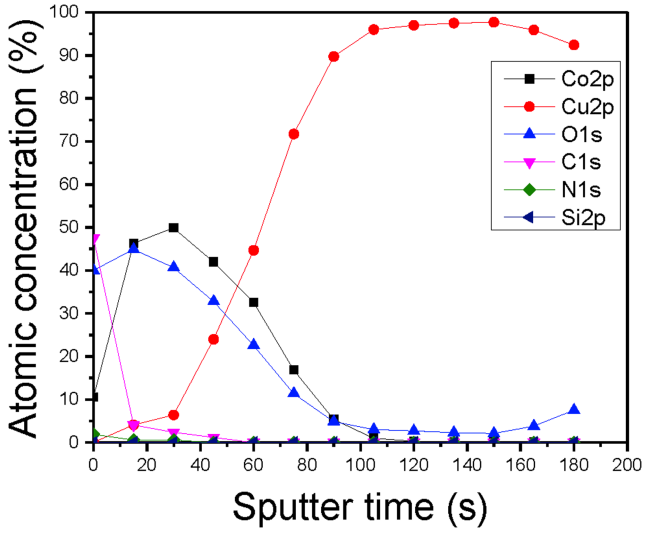

FIG. 5. Plot of atomic concentration versus argon ion sputtering time of a 14 nm thick cobalt film grown on a copper substrate at 180 °C.

with the cobalt metal to afford copper metal and cobalt oxide. This reduction process could lead to the observed intermixing. The element concentrations in Fig. 5 suggest both cobalt and copper in the 14 nm thick layer with little copper at the surface of the film. The copper concentration increases with depth in the cobalt-containing layer. In related work, Gordon reported that a continuous, electrically connected 1.4 nm thick copper film could be grown by ALD at 190 °C on a 2 nm thick ALD cobalt layer.[38,63] Ekerdt also reported that the ALD growth of cobalt metal films on copper substrates using $Co(tBuNCEtNtBu)_2$ and H_2 at 265 °C led to intermixing of the copper and cobalt, and a surfactant-like copper layer ~2 nm thick was observed on top of the cobalt layer up to 16 nm film thicknesses.[64] Unlike Ekerdt's work, we did not observe a copper surface layer by XPS, perhaps because of the presence of the copper oxides at initial stages of growth or because of our lower 180 °C growth temperature. Prior to deposition, Ekerdt removed the copper oxide layer on the copper substrate by treatment with glacial acetic acid, presumably to afford a pristine copper metal surface. Accordingly, nucleations in the work of Ekerdt[64] and Gordon[38,63] are likely facilitated by the interfacial metallic cobalt-copper alloy formation. Our substrates were not treated with acetic acid prior to depositions, so it is not clear if our nucleations on copper are promoted by interfacial metallic alloy formation or by reduction of the surface copper oxides by the cobalt metal.

B. Attempted film growth on Si(100) with native oxide, Si–H, and CDO substrates

As a part of the selectivity studies, cobalt metal ALD was attempted on Si(100), Si–H, and CDO substrates, using the conditions described above for growth on metal substrates. No film growth was observed by SEM on any of these substrates at up to 1000 cycles, and EDS revealed no signals for cobalt in any of the samples. Additionally, a CDO substrate was subjected to 150 cycles of ALD cobalt metal growth conditions at 180 °C as described above. The CDO substrate was then analyzed by XPS to determine if there was any cobalt metal on the surface. Inspection of the Co 2p region showed no ionizations for any cobalt species. The CDO substrate surface only showed the expected ionizations for carbon, silicon, and oxygen. Accordingly, cobalt metal does not nucleate on Si(100), Si–H, and CDO surfaces using **1** and formic acid at 180 °C.

C. Film growth on thermal SiO_2 substrates

Unlike Si(100), Si–H, and CDO substrates, attempted ALD growth of cobalt metal films from **1** and formic acid at 180 °C on 100 nm thermal SiO_2/Si(100) substrates led to the growth of continuous films. These films were non-conductive and did not show the metallic sheen of cobalt metal films. Films grown with 500 cycles were 35 nm thick, but were also 35 nm thick after 1000 cycles, suggesting a very different behavior than the cobalt metal growth on metallic substrates described above. EDS analysis of a 35 nm thick film grown with 500 cycles showed a cobalt signal, indicating that the layer contained cobalt. The substrate with the 35 nm thick film grown with 500 cycles was rinsed with deionized water and was then blown dry with a stream of clean, dry air. Subsequent SEM analysis showed that the film had completely dissolved and only the thermal SiO_2 layer was observed. This experiment demonstrates that the material deposited on SiO_2 is water soluble. For comparison, 25 nm thick cobalt metal films on ruthenium, platinum, and copper substrates were unaffected by rinses with deionized water. A 35 nm thick film on thermal SiO_2 was probed with infrared spectroscopy and showed absorptions at 1574 and 1349 cm^{-1}, in addition to the SiO_2 absorptions. For comparison, a commercial sample of anhydrous copper(II) formate tetrahydrate showed absorptions at 1551 and 1359 cm^{-1}. Sodium formate shows carbon-oxygen stretches in the infrared spectrum at 1567 and 1366 cm^{-1}.[65] Finally, a 35 nm thick film on thermal SiO_2 was rinsed with deionized water to dissolve the film, dried with a stream of clean, dry air, and then subjected to analysis by infrared spectroscopy. The absorptions at 1574 and 1349 cm^{-1} were not present on the water-rinsed substrate. These observations are consistent with the formation of cobalt(II) formate on the thermal SiO_2 substrates. The fact that cobalt(II) formate layers grow only on the 100 nm thick thermal SiO_2 substrates, and not on Si(100) with native oxide (1-2 nm), must be related to reactions of the thick SiO_2 layer with formic acid, which then lead to cobalt(II) formate upon subsequent treatment with **1**. There is not enough SiO_2 on Si(100) with native oxide substrates to afford detectable amounts of cobalt(II) formate.

D. ALD selectivity temperature window

We next sought to define the "area-selective ALD temperature window," which is the temperature range where inherent selectivity for metal surfaces is observed but no growth occurs on dielectric surfaces. Depositions were carried out with the pulse sequence described above, but the substrate temperatures were varied to determine the temperature dependence of the selective ALD processes. Since <20 nm thick cobalt metal films are desired in device fabrication, each deposition was run with 250 cycles (~25 nm thick films on metal substrates). Depositions were performed at 160, 170, 180, 190, 200, and 220 °C on Si(100), Si–H, and CDO substrates to observe the temperature at which nucleation begins to occur. Temperatures of 230 °C and higher were avoided, since self-decomposition of **1** to cobalt metal occurs.[56] No film growth was observed by

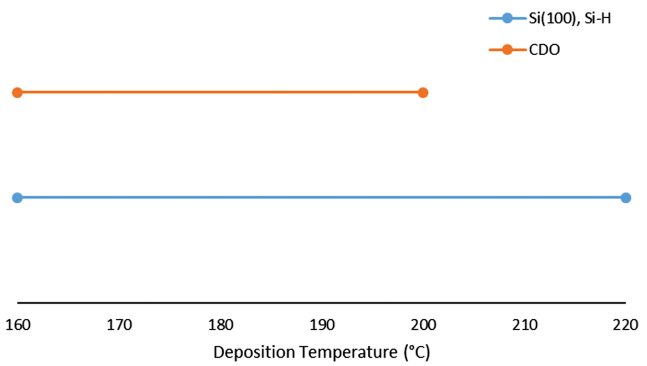

FIG. 6. Area-selective ALD temperature windows, where no growth was observed on Si(100), Si–H, and CDO substrates after 250 cycles.

SEM from 160 to 200 °C on any of the substrates. At 220 °C, no film growth was detected on Si(100) or Si–H; however, CDO showed the formation of particles on the surface. Attempts were made to characterize the surfaces of the CDO substrates containing the particles that were deposited at 220 °C. No cobalt signals were observed with EDS, which is consistent either with the particles not containing cobalt or, more likely, with insufficient signal to noise to observe the cobalt EDS signal from widely spaced particles. Therefore, cobalt metal films from **1** and formic acid have a substrate selectivity temperature window for growth on metals and not on CDO from 160 to 200 °C (Fig. 6). The selectivity window for growth on metals over Si(100) and Si–H spans 160–220 °C (Fig. 6). SiO_2 substrates are a special case, since cobalt(II) formate appears to form on these surfaces at 180 °C.

IV. CONCLUSIONS

This work describes the initial stages of cobalt metal growth by ALD from precursors **1** and formic acid at 180 °C on ruthenium, platinum, copper, Si(100), Si–H, SiO_2, and CDO substrates. On platinum and copper substrates, plots of thickness versus number of growth cycles were linear between 25 and 250 cycles, with a growth rate of 0.98 Å/cycle. This growth rate is the same as that on ruthenium between 250 and 2000 cycles, suggesting rapid nucleation on platinum and copper substrates and normal growth by 25 cycles (~2.5 nm thick cobalt layers). By contrast, growth on ruthenium substrates showed a delay of up to 250 cycles before a saturative growth rate was observed. No films were observed after 25 and 50 cycles by SEM. Between 100 and 150 cycles, a rapid growth rate of ~1.6 Å/cycle was observed, which suggests that a CVD-like growth occurs until the surface is covered with ~10 nm of cobalt metal. Normal ALD growth ensues after 250 cycles. AFM showed smooth, continuous cobalt metal films on platinum substrates after 150 cycles (~14 nm thick) with an rms surface roughness of 0.6 nm. Cobalt metal films grown on copper substrates with 150 cycles (~14 nm thick) had rms surface roughnesses of 1.1–2.4 nm after 150 cycles with 30–125 nm diameter particles and 30–60 nm diameter pits that were also present on the uncoated copper substrates. Based upon XPS analyses and previous reports, the rapid nucleation of the cobalt metal on platinum substrates appears to occur through the formation of interfacial cobalt-platinum alloys. Nucleation of cobalt on copper substrates is less clear, but may occur through reduction of surface copper oxides by the growing cobalt film or may also entail cobalt-copper interfacial alloy formation. Films grown on ruthenium, platinum, and copper substrates showed resistivities of <20 $\mu\Omega$ cm after 250 cycles and had values close to those of the uncoated substrates at ≤150 cycles. No film growth was observed after 1000 cycles on Si(100), Si–H, and carbon-doped oxide substrates. Growth on thermal SiO_2 substrates afforded ~35 nm thick layers after ≥500 cycles. This layer is proposed to be cobalt(II) formate, based upon its water solubility, insulating nature, and infrared spectrum. Selective deposition of cobalt metal on metallic substrates over Si(100), Si–H, and CDO was observed from 160 to 200 °C. Particle deposition was observed on CDO substrates at 220 °C.

SUPPLEMENTARY MATERIAL

See supplementary material for film growth and characterization data.

ACKNOWLEDGMENTS

The authors gratefully acknowledge generous financial support from the U.S. National Science Foundation (Grant Nos. CHE-1212574 and CHE-1607973 to C.H.W. and CHE-1300180 to Y.J.C.) and EMD Performance Materials. U.S. National Science Foundation Grant Nos. CHE-1427926 and DMR-0922912 are also acknowledged for the purchase of a powder X-ray diffractometer and a field emission SEM, respectively. Jean-Francois Veyan is acknowledged for his advice and assistance with the acquisition and interpretation of the XPS data.

[1] L. V. Lutsev, A. I. Stognij, and N. N. Novitskii, Phys. Rev. B **80**, 184423 (2009).
[2] C. Vo-Van, Z. Kassir-Bodon, H. Yang, J. Coraux, J. Vogel, S. Pizzini, P. Bayle-Guillemaud, M. Chshiev, L. Ranno, V. Guisset, P. David, V. Salvador, and O. Fruchart, New J. Phys. **12**, 103040 (2010).
[3] S. Zhu, R. L. Van Meirhaeghe, C. Detavernier, F. Cardon, G.-P. Ru, X.-P. Qu, and B.-Z. Li, Solid-State Electron. **44**, 663–671 (2000).
[4] M. He, X. Zhang, T. Nogami, X. Lin, J. Kelly, H. Kim, T. Spooner, D. Edelstein, and L. Zhao, J. Electrochem. Soc. **160**, D3040–D3044 (2013).
[5] C.-C. Yang, P. Flaitz, P. C. Wang, F. Chen, and D. Edelstein, IEEE Electron Device Lett. **31**, 728–730 (2010).
[6] Y. Kokaze, S. Kodaira, Y. Endo, J. Hamaguchi, M. Harada, S. Kumamoto, Y. Sakamoto, and Y. Higuchi, Jpn. J. Appl. Phys. **52**, 05FA01 (2013).
[7] M. Wislicenus, R. Liske, L. Gerlich, B. Vasilev, and A. Preusse, Microelectron. Eng. **137**, 11–15 (2015).
[8] A. H. Simon, T. Bolom, C. Niu, F. H. Baumann, C.-K. Hu, C. Parks, J. Nag, H. Kim, J. Y. Lee, C.-C. Yang, S. Nguyen, H. K. Shobha, T. Nogami, S. Gugglia, J. Ren, D. Sabens, and J. F. AuBuchon, *2013 IEEE International Reliability Physics Symposium (IRPS)* (IEEE, 2013), pp. 3F.4.1-3F.4.6.
[9] M. Lapedus, Semiconductor Engineering, 2015, http://semiengineering.com/interconnect-challenges-grow-2/.
[10] P. McLellan, Cadence, 2016, https://community.cadence.com/cadence_blogs_8/b/breakfast-bytes/archive/2016/06/24/an-steegen-16.
[11] W.-Z. Xu, J.-B. Xu, H.-S. Lu, J.-X. Wang, Z.-J. Hu, and X.-P. Qu, J. Electrochem. Soc. **160**, D3075–D3080 (2013).
[12] H. Ago, Y. Ito, N. Mizuta, K. Yoshida, B. Hu, C. M. Orofeo, M. Tsuji, K.-I. Ikeda, and S. Mizuno, ACS Nano **4**, 7407–7414 (2010).
[13] R. M. H. New, R. F. W. Pease, and R. L. White, J. Vac. Sci. Technol., B: Microelectron. Nanometer Struct. **12**, 3196–3201 (1994).
[14] J. A. Hamilton, T. Pugh, A. L. Johnson, A. J. Kingsley, and S. P. Richards, Inorg. Chem. **55**, 7141–7151 (2016).
[15] T. J. Knisley, L. C. Kalutarage, and C. H. Winter, Coord. Chem. Rev. **257**, 3222–3231 (2013).
[16] T. Pugh, S. D. Cosham, J. A. Hamilton, A. J. Kingsley, and A. L. Johnson, Inorg. Chem. **52**, 13719–13729 (2013).
[17] J. Kwon, M. Saly, R. K. Kanjolia, and Y. J. Chabal, Chem. Mater. **23**, 2068–2074 (2011).
[18] M. F. Chioncel and P. W. Haycock, Chem. Vap. Deposition **11**, 235–243 (2005).
[19] M. A. Paranjape, A. U. Mane, A. K. Raychaudhuri, K. Shalini, S. A. Shivashankar, and B. R. Chakravarty, Thin Solid Films **413**, 8–15 (2002).
[20] P. A. Lane, P. E. Oliver, P. J. Wright, C. L. Reeves, A. D. Pitt, and B. Cockayne, Chem. Vap. Deposition **4**, 183–186 (1998).
[21] S. M. George, Chem. Rev. **110**, 111–131 (2010).
[22] M. Leskelä and M. Ritala, Angew. Chem., Int. Ed. **42**, 5548–5554 (2003).
[23] M. Putkonen and L. Niinistö, Top. Organomet. Chem. **9**, 125–145 (2005).
[24] J.-H. Park, D.-Y. Moon, D.-S. Han, Y.-J. Kang, S.-R. Shin, H.-T. Jeon, and J.-W. Park, Surf. Coat. Technol. **259**, 98–101 (2014).

[25]J. Park, H.-B.-R. Lee, D. Kim, J. Yoon, C. Lansalot, J. Gatineau, H. Chevrel, and H. Kim, J. Energy Chem. **22**, 403–407 (2013).
[26]H. Kim, Microelectron. Eng. **106**, 69–75 (2013).
[27]H.-B.-R. Lee, Y. J. Park, S. Baik, and H. Kim, Chem. Vap. Deposition **18**, 41–45 (2012).
[28]J. Yoon, H.-B.-R. Lee, D. Kim, T. Cheon, S.-H. Kim, and H. Kim, J. Electrochem. Soc. **158**, H1179–H1182 (2011).
[29]J.-M. Kim, H.-B.-R. Lee, C. Lansalot, C. Dussarat, J. Gatineau, and H. Kim, Jpn. J. Appl. Phys. **49**, 05FA10 (2010).
[30]K. Lee, K. Kim, T. Park, H. Jeon, Y. Lee, J. Kim, and S. Yeom, J. Electrochem. Soc. **154**, H899–H903 (2007).
[31]K. Kim, K. Lee, S. Han, T. Park, Y. Lee, J. Kim, S. Yeom, and H. Jeon, Jpn. J. Appl. Phys. **46**, L173–L176 (2007).
[32]K. Kim, K. Lee, S. Han, W. Jeong, and H. Jeon, J. Electrochem. Soc. **154**, H177–H181 (2007).
[33]H.-B.-R. Lee and H. Kim, Electrochem. Solid-State Lett. **9**, G323–G325 (2006).
[34]H. B. Profijt, S. E. Potts, M. C. M. van de Sanden, and W. M. M. Kessels, J. Vac. Sci. Technol., A **29**, 050801 (2011).
[35]B. S. Lim, A. Rahtu, and R. G. Gordon, Nat. Mater. **2**, 748–754 (2003).
[36]B. S. Lim, A. Rahtu, J.-S. Park, and R. G. Gordon, Inorg. Chem. **42**, 7951–7958 (2003).
[37]Z. Li, D. K. Lee, M. Coulter, L. N. J. Rodriguez, and R.G. Gordon, Dalton Trans. 2592–2597 (2008).
[38]Z. Li, R. G. Gordon, D. B. Farmer, Y. Lin, and J. Vlassak, Electrochem. Solid-State Lett. **8**, G182–G185 (2005).
[39]T. D.-M. Elko-Hansen and J. G. Ekerdt, Chem. Mater. **26**, 2642–2646 (2014).
[40]H.-B.-R. Lee and H. Kim, ECS Trans. **16**, 219–225 (2008).
[41]H.-B.-R. Lee, W.-H. Kim, J. W. Lee, J.-M. Kim, K. Heo, I. C. Hwang, Y. Park, S. Hong, and H. Kim, J. Electrochem. Soc. **157**, D10–D15 (2010).
[42]H.-B.-R. Lee, J. Kim, H. Kim, W.-H. Kim, J.-W. Lee, and I. Hwang, J. Korean Phys. Soc. **56**, 104–107 (2010).
[43]J. Kwon, M. Saly, M. D. Halls, R. K. Kanjolia, and Y. J. Chabal, Chem. Mater. **24**, 1025–1030 (2012).
[44]L. C. Kalutarage, P. D. Martin, M. J. Heeg, and C. H. Winter, J. Am. Chem. Soc. **135**, 12588–12591 (2013).
[45]A. J. M. Mackus, A. A. Bol, and W. M. M. Kessels, Nanoscale **6**, 10941–10960 (2014).
[46]W.-H. Kim, F. S. M. Hashemi, A. J. M. Mackus, J. Singh, J. Kim, D. Bobb-Semple, Y. Fan, T. Kaufman-Osborn, L. Godet, and S. F. Bent, ACS Nano **10**, 4451–4458 (2016).
[47]B. Kalanyan, P. C. Lemaire, S. E. Atanasov, M. J. Ritz, and G. N. Parsons, Chem. Mater. **28**, 117–126 (2016).
[48]F. S. M. Hashemi, C. Prasittichai, and S. F. Bent, ACS Nano **9**, 8710–8717 (2015).
[49]X. Jiang, H. Wang, J. Qi, and B. G. Willis, J. Vac. Sci. Technol., A **32**, 041513 (2014).
[50]E. Färm, M. Kemell, M. Ritala, and M. Leskelä, Chem. Vap. Deposition **12**, 415–417 (2006).
[51]K. J. Park, J. M. Doub, T. Gougousi, and G. N. Parsons, Appl. Phys. Lett. **86**, 051903 (2005).
[52]C.-C. Yang, F. Baumann, P.-C. Wang, S. Y. Lee, P. Ma, J. AuBuchon, and D. Edelstein, Microelectron. Eng. **106**, 214–218(2013).
[53]S. W. Ryu, S. Kim, J. Yoon, J. T. Tanskanen, H. Kim, and H.-B.-R. Lee, Curr. Appl. Phys. **16**, 88–92 (2016).
[54]J. P. Klesko, M. M. Kerrigan, and C. H. Winter, Chem. Mater. **26**, 700–703 (2016).
[55]https://en.wikipedia.org/wiki/Cobalt. See also J. A. Dean, *Lange's Handbook of Chemistry*, 15th ed. (McGraw-Hill, 1999), Section 4, Table 4.1.
[56]T. J. Knisley, M. J. Saly, M. J. Heeg, J. L. Roberts, and C. H. Winter, Organometallics **30**, 5010–5017 (2011).
[57]J. Hämäläinen, M. Ritala, and M. Leskelä, Chem. Mater. **26**, 786–801 (2014).
[58]D. Adner, M. Korb, S. Schulze, M. Hietschold, and H. Lang, Chem. Commun. **48**, 6855–6857 (2013).
[59]J. A. Aboaf, S. R. Herd, and E. Klokholm, IEEE Trans. Magn. **19**, 1514–1519 (1983).
[60]L. C. Kalutarage, S. B. Clendenning, and C. H. Winter, Chem. Mater. **26**, 3731–3738 (2014).
[61]I. J. Hsu, B. E. McCandless, C. Weiland, and B. G. Willis, J. Vac. Sci. Technol., A **27**, 660–667 (2009).
[62]B. G. Willis, J. Qi, J. Chen, G. J. Weisel, and D. T. Zimmerman, ECS Trans. **64**, 253–263 (2014).
[63]Z. Li, A. Rahtu, and R. G. Gordon, J. Electrochem. Soc. **153**, C787–C794 (2006).
[64]T. D.-M. Elko-Hansen, A. Dolocan, and J. G. Ekerdt, J. Phys. Chem. Lett. **5**, 1091–1095 (2014).
[65]K. Ito and H. J. Bernstein, Can. J. Chem. **34**, 170–178 (1956).